

Three-dimensional simulation of regional urban waterlogging based on high-precision DEM model

Zipeng Chen

Zhongnan University of Economics and Law - Nanhu Campus: Zhongnan University of Economics and Law

Kun Li (✉ li_kunf@stu.zuel.edu.cn)

Zhongnan University of Economics and Law - Nanhu Campus: Zhongnan University of Economics and Law <https://orcid.org/0000-0003-2888-8745>

Jianhua Du

Zhongnan University of Economics and Law - Nanhu Campus: Zhongnan University of Economics and Law

Yi Chen

Zhongnan University of Economics and Law - Nanhu Campus: Zhongnan University of Economics and Law

Ronggang Liu

Zhongnan University of Economics and Law - Nanhu Campus: Zhongnan University of Economics and Law

Yi Wang

Zhongnan University of Economics and Law - Nanhu Campus: Zhongnan University of Economics and Law

Manuscript

Keywords: urban waterlogging, high-precision DEM model, three-dimensional GIS, disaster simulation

Posted Date: February 10th, 2021

DOI: <https://doi.org/10.21203/rs.3.rs-208624/v1>

License:  This work is licensed under a Creative Commons Attribution 4.0 International License.

[Read Full License](#)

Three-dimensional simulation of regional urban waterlogging based on high-precision DEM model

Author 1

- Zipeng Chen
- School of Information and Safety Engineering, Zhongnan University of Economics and Law, Wuhan 430074, China

Author 2

- Kun Li
- School of Information and Safety Engineering, Zhongnan University of Economics and Law, Wuhan 430074, China

Author 3

- Jianhua Du
- School of Information and Safety Engineering, Zhongnan University of Economics and Law, Wuhan 430074, China

Author 4

- Yi Chen
- School of Information and Safety Engineering, Zhongnan University of Economics and Law, Wuhan 430074, China

Author 5

- Ronggang Liu
- School of Information and Safety Engineering, Zhongnan University of Economics and Law, Wuhan 430074, China

Author 6

- Yi Wang
- School of Information and Safety Engineering, Zhongnan University of Economics and Law, Wuhan 430074, China

*Correspondence: li_kunf@stu.zuel.edu.cn

Abstract: In order to deal with the urban waterlogging disasters, a high precision three-dimensional (3D) Digital Elevation Model (DEM) is built in this paper. This DEM is based on high-precision data of urban topography and geomorphology, covering 3D surface elevation, road network and structures. The simulation calculation of this model can get different watershed area according to different elevation based on the topographic feature. Furthermore, divide the urban regional model into the stage sub-catchment area corresponding to the elevation. Within the sub-catchment area, it can also reflect the situation of urban waterlogging, in combination with the rainstorm intensity formula, the statistics of local area underlying surface, and Soil Conservation Service (SCS) model of runoff simulation. It can also help to simulate the submergence depth and range under different recurrence stages of rainfall scenarios. The research shows that this DEM model can provide the premise for the highly accurate numerical simulation of surface runoff and confluence, which can effectively improve the accuracy of the division of catchment area and the assessment, prediction of waterlogging disaster. This provides an important idea and method for the flood prevention and control in flood season for reservoir, tailings pond and urban waterlogging.

Keywords: urban waterlogging, high-precision DEM model, three-dimensional GIS, disaster simulation

Declarations:

Funding: This article has no supported funding.

Conflicts of interest/Competing interests: There is no conflicts of interest or competing interests.

Availability of data and material: If it is needed, the data can be available.

Code availability: If it is needed, the data can be available.

1 **1. Introduction**

2 With the increase of the cities' area and the appearance of big cities, the landform of cities has been changed. According
3 to the statics, the area of lakes in the southern cities of China cities has reduced by 50 percent in the past seventy or eighty
4 years. Taking Wuhan for example, from 1987 to 2016, the area of lakes in Wuhan's main urban area shrank by a total of
5 128.28 km², and the closer it is to the urban building area, the more obviously the lake area shrank; the smaller the lake
6 area, the more filling phenomenon [1]. In addition, the change of urban geomorphology has broken the balance of rainfall
7 and evaporation and the frequency of extreme weather caused by global climate change has increased in recent years. Due
8 to these two reasons, urban waterlogging has become a common disease in many southern cities in the rainy season. The
9 domestic waterlogging situation in recent years is as shown in Table 1. Many urban waterlogging cases show that urban
10 waterlogging disasters with regional characteristics, which happens at city small low-lying area. So studying the distribution
11 of regional waterlogging in different rainfall recurrence and generating strategy of preventing waterlogging is of important
12 value to reducing the economic loss and improving residents' life and property safety.

13 **Tab.1 Urban waterlogging of Chinese cities in recent years**

| Year | Disaster Region | Total Rainfall(mm) | Loss (¥100 million) |
|------|------------------|--------------------|---------------------|
| 2013 | Sichuan Province | 170 | 53.7 |
| 2014 | Shenzhen | 318 | 0.8 |
| | Hunan Province | 315.2 | 25.8 |
| 2015 | Wuhan | 197 | 0.68 |
| 2016 | Wuhan | 560.5 | 22.65 |
| 2017 | Hunan Province | 435 | 385.1 |
| 2018 | Chengdu | 306.4 | 24 |

14 *Significance and Novelty of This Research*

15 In recent years, with the development of computer science, some scholars firstly put forward models such as SWMM,
16 UCURM, MOUSE, STORM and WALLINFORD, all of which have achieved good application effects [2-4]. In China,
17 Chinese scholars have also made many efforts. For example, simulation system of rainstorm waterlogging in Tianjin City
18 developed by Qiu and others in 2000, based on the two-dimensional unsteady hydraulics model and combined with the
19 monitoring of rainfall information, simulated urban waterlogging, which is the first well-known waterlogging simulation
20 system in China [5,6]. But its spatial analysis ability is weak. Later, Wang established an urban waterlogging disaster
21 analysis model by using GIS in 2004, which further solved the problems encountered by Qiu [7]. Since then, the study of
22 waterlogging in China has entered an era of rapid development. Scholars have combined GIS with various waterlogging
23 models and verified them in big cities, which achieved good results. For example, Ye constructed flood inundation model
24 and established urban road-waterlogging-zone map [8]. Jing carried out risk analysis of waterlogging disaster simulation
25 by GIS technology [9]. However, in most of the previous studies, the research areas are mostly large-scale areas. In 2010,

26 Yin proposed a small-scale urban waterlogging simulation, which shrank the study area form an entire city to a single
27 administrative region, while no more small-scale waterlogging simulation was carried out [10]. By combining the rule of
28 urban waterlogging occurred in recent years, the influenced area of waterlogging is usually small. While the simulation
29 precision of waterlogging in large-scale region is not enough, which is unable to locate precisely to disaster area. And the
30 DEM data used is often 30m by 30m raster data, which cannot construct a high precision terrain model. However, in the
31 study of waterlogging, DEM model is the foundation of dividing catchment area and simulate the runoff.

32 To sum up, it can be seen that the current urban waterlogging simulation methods are mainly combined with spatial
33 geographic information, rainfall and urban drainage pipe network to simulate the surface runoff and confluence process,
34 which have been relatively mature. However, the research areas are mostly large areas, and there are few researches on
35 waterlogging in small areas such as factories and schools. In addition, on the issue of dividing catchment area, the previous
36 research is mostly based on drainage pipe network, no actual consideration of terrain characteristics. In this paper, watershed
37 is extracted according to high-precision DEM model and topographic features, which divide the study area to different
38 catchment areas. And simulate the disasters in each area. Finally, three-dimensional visualization technology is used to
39 display the simulation results. This method can be used to understand the disaster in the region more intuitively and
40 accurately. This paper further expands the research ideas and methods of urban waterlogging disaster, and provides
41 reference for the simulation and early warning of waterlogging in small areas.

42 **2. Research ideas and methods**

43 High-precision 3D DEM data is an important data basis for the study, in order to ensure the model accuracy and
44 facilitate the high-precision topographic mapping. The research area of this paper is located in Zhongnan University of
45 Economics and Law, Wuhan, China. This area is low-lying and waterlogging disasters occur in every year's rainstorm
46 season, especially in 2016. As shown in Figure 1, waterlogging depth in the building exceeds 50cm, resulting in a loss of
47 2.36 million of equipment caused by flooding.



48
49 **Figure 1. The condition of waterlogging in 2016**

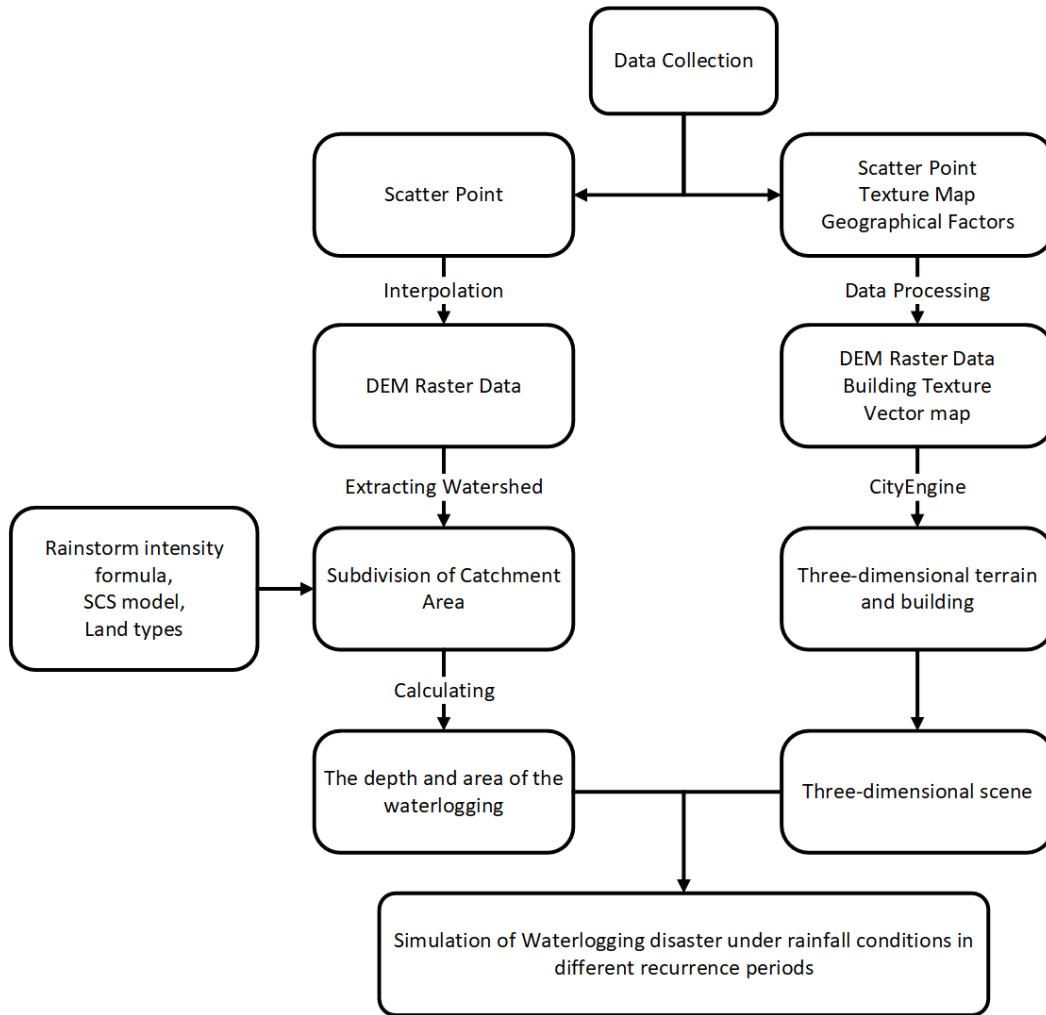
50 **2.1 Overview of the model area**

51 Wuhan, located in central China, has a humid north subtropical monsoon climate with abundant rainfall, sunshine, hot
52 summer and cold winter. There is more rainfall in the plum rain season in early summer. The annual rainfall is 1100 mm.

53 The waterlogging prone season is from June to August. This paper takes Zhongnan University of Economics and Law as
 54 study area. The total area of the study area is 1.11km^2 , and the land types are mainly divided into building land, road,
 55 grassland and lake. There are 67 buildings, covering a total area of 0.49km^2 , including two teaching buildings, 8
 56 administrative office buildings, 17 dormitory buildings for students and 16 dormitory buildings for teachers. Roads,
 57 greenery and lakes cover an area of 0.49km^2 , 0.20km^2 and 0.11km^2 respectively.

58 2.2 Study framework

59 The study framework of this 3D DEM urban waterlogging model simulation is shown in Figure 2.



60
61 **Figure 2. Framework of waterlogging simulation**

62 2.3 The watershed extraction method

63 The watershed is the basis for dividing the catchment area. The runoff on both sides of the watershed flows in their
 64 respective areas and cannot be collected. Based on high-precision DEM data and the flood simulation method from bottom
 65 to top of surface elevation difference, the boundary of different sub-catchment areas can be found, the watershed of the
 66 study area is extracted automatically, and then the catchment area is delimited.

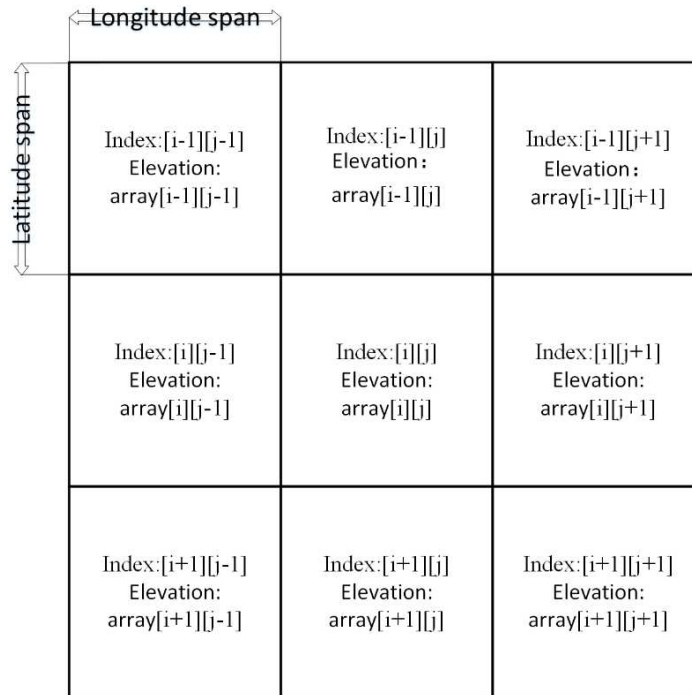
67 2.3.1 High precision terrain model

68 In order to ensure the accuracy of the data, the millimeter-level GPS measuring instrument was used to obtain the

69 elevation data points. After field measurement, artificial modification and expansion are carried out according to the actual
 70 terrain to generate a 0.7m×0.7m High-precision DEM model.

71 **2.3.2 Automatic watershed extraction method**

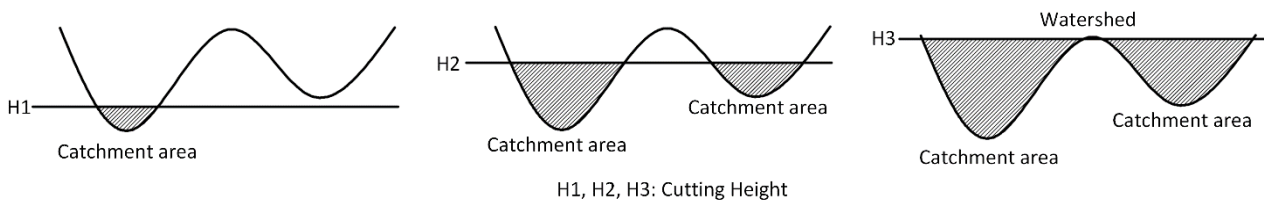
72 In the computer, we can read DEM raster data into a two-dimensional array, each raster has a unique identification,
 73 and each value in the array is the elevation value of the raster. The raster data principle is shown in Figure 3.



74

75 **Figure 3. Principle of grid data**

76 Watershed extraction algorithm is to use different height of the plane to cut raster data to find the region lower than
 77 the plane. As the cutting plane is raised continuously, the number and range of areas will increase continuously. When two
 78 or more regions are about to intersect, because the terrain is continuously changing, we can get a continuous boundary, and
 79 the boundary is the watershed of the research area. The study area is divided into several sub-catchment areas. The principle
 80 is shown in Figure 4.



81

82 **Figure 4. Principle of extracting watershed**

83 Watershed extraction algorithm is implemented by Python programming. The algorithm flow is described as follows:

84 (1) Read the DEM raster array. Find the minimum and maximum values in the array. Define the starting and ending
 85 height of the cutting plane and a new catchments array to hold the region which is lower than the cutting plane found in the

86 loop. Define a new array which have the same number of rows and columns as the original grid array to save the watershed.

87 (2) Define the cutting height as the starting height, judge whether the cutting height is less than or equal to the ending
88 height, and then enter the loop.

89 (3) After entering the loop, traverse the original raster array. If the elevation value of a point is less than or equal to the
90 cutting height, change the value of that point in the catchment area array, and find the region under the cutting height.

91 (4) Traverse each point in the catchment area array, iterate through the points in the certain area in 8 directions, and
92 divide different areas with different numbers.

93 (5) Traversing the array of catchment areas, if there are points of two regions in the eight grids around a certain point,
94 the point is the point in the watershed of two regions, and the point is saved in the watershed array.

95 (6) As the cutting height increases, judge whether the cutting height is less than or equal to the termination height; if
96 it is true, continue the loop (3) - (5); if not, jump out of the loop and cut the original raster data according to the index value
97 of the watershed array, and output the array of sub-catchment areas after cutting.

98 2.4 Urban waterlogging disaster model

99 2.4.1 The rainstorm intensity formula

100 The rainstorm intensity formula is the premise to study urban waterlogging disaster. According to the Design
101 Specification for Outdoor Drainage, the formula of rainstorm intensity is defined as follows:

$$102 \quad q = \frac{167A(1 + C \lg p)}{(t + b)^n} \quad (1)$$

103 Where: Q is the intensity of the storm, $L/s \cdot hm^2$; A is rainfall, mm ; C is the variation parameter of rainfall, which is
104 one of the parameters reflecting the variation degree of rainfall intensity in different recurrence periods; P is the designed
105 rainfall recurrence period, a ; T is rainfall duration, min ; b and n are constants, which reflect the changes of rainfall
106 intensity over time.

107 2.4.2 The SCS model

108 The SCS model is based on the basic assumption that the ratio of the actual infiltration capacity to the potential storage
109 capacity of catchment area is equal to the ratio of the actual surface runoff volume to the maximum possible runoff volume
110 of catchment area, which can be expressed as Formula 2.

$$111 \quad \frac{F}{S} = \frac{R}{P - I_a} \quad (2)$$

112 Where: R is the runoff, mm ; P is rainfall, mm ; I_a is the initial lower volume, mm , including closure, surface water
113 storage, etc. F cumulative infiltration, mm ; S is the maximum possible stagnant flow in the basin, mm .

114 The relationship between the initial loss and the maximum retention can be expressed as a first-order linear relationship,
115 and the relationship between the two is verified by the U.S. Soil Conservation Service through a large amount of rainfall
116 data, as shown in Equation 3.

117
$$I_a = 0.2S \quad (3)$$

118 Then according to the principle of water balance, the calculation formula of runoff is shown in Formula 4.

119
$$R = \frac{(P - 0.2S)^2}{P + 0.8S} \quad (4)$$

120 To calculate the maximum retention S, the parameter CN is brought in. The value of CN is only related to the soil type
121 and land type under the basin. The relationship between the two is shown in Equation 5.

122
$$S = \frac{25400}{CN} - 254 \quad (5)$$

123 The value of CN is generally an integer less than 100. It can be seen from the above formula that the greater CN is,
124 the greater the runoff will be generated. The CN values corresponding to different land types can be obtained by looking
125 up the table.

126 **2.4.3 The process of confluence disaster**

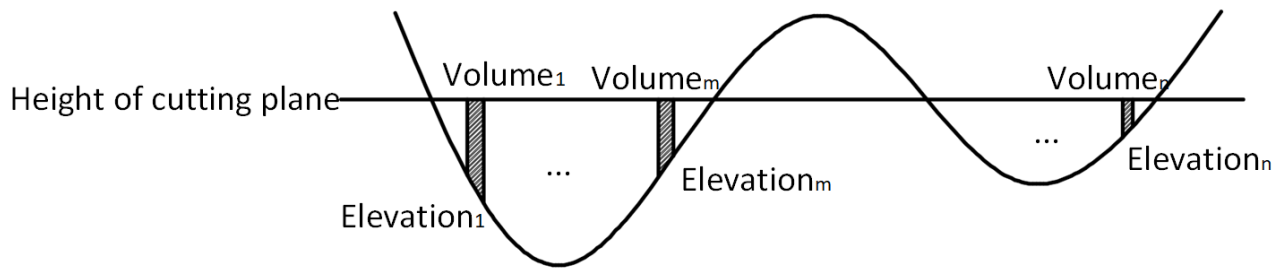
127 After the rain falls, it first passes through the interception of plants, the storage of depressions and the infiltration in
128 soil. When the rainfall makes the natural storage saturated, the rain starts to flow along the surface slope. If the rainfall
129 continues to increase, the scope of the diffuse flow will also increase, forming a comprehensive diffuse flow. Under the
130 influence of gravity, water flows to the lower terrain and gather, then enters the urban drainage pipe network. When the
131 urban drainage pipe network is unable to discharge all the runoff generated by rainfall, that is when the runoff volume is
132 greater than the displacement volume, waterlogging disasters will occur in the lower terrain. The numerical difference
133 between the runoff volume and the displacement volume is the disaster-causing volume, and the relationship among the
134 above three factors can be expressed in Formula 6.

135
$$W = R * S_1 - D * S_2 \quad (6)$$

136 Where: R is the runoff of rainwater, *mm*; S_1 is runoff area, mm^2 ; W is the amount of disaster, *mm*; D is the
137 ability of underground drainage system capacity system, *mm/h*; S_2 is the drainage area, mm^2 .

138 **2.4.4 The calculation of submergence depth**

139 For a sub-catchment area, it can be considered as a container whose height of the water corresponds to the volume of
140 the water. That is to say, for a certain disaster-causing volume W, there is a corresponding submergence depth H in the
141 catchment area. Based on the certain disaster-causing volume, the water volume of each grid in the DEM raster data of
142 different heights can be calculated, and then the total water volume can be obtained by summation. The volumetric principle
143 of DEM raster data is shown in Figure 5.



144

145

Figure 5. Principle of calculating the volume of DEM data

146

The volume calculation formula is as follows in Formula 7:

147

$$V = \sum_{i=1}^n S_{cell} * (H - h_i) \quad (7)$$

148

Where V is the volume under fixed height, S_{cell} is the grid area, H is the fixed cutting height, and h_i is the i^{th} grid elevation value.

149

150

Under a certain disaster-causing volume W , the lowest point was set as the initial cutting height H . If $W > V$, the step length was increased to 0.01m. When the difference between W and V was the smallest, H was the height of the cutting plane, and $H - h_{min}$ was the maximum waterlogging depth of the region.

152

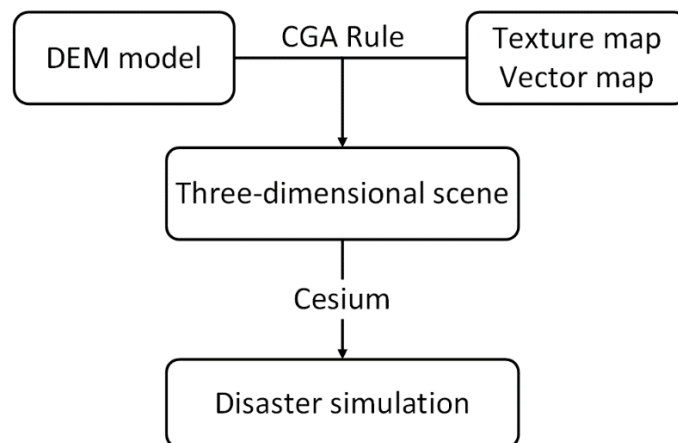
153

2.5 3D dimensional visual simulations

154

The technical system of 3D modeling and disaster simulation in this paper mainly includes CityEngine and Cesium, and the simulation steps are shown in Figure 6.

155



156

157

Figure 6. Framework of 3-dim visualization

158

CityEngine is a three-dimensional software to construct models, which has the following characteristics:

159

(1) With high modeling efficiency, CityEngine has a set of unique rules modeling methods, which can change the modeling process into a code writing process, making it convenient and fast.

160

161

(2) With strong compatibility, model files generated by ArcGIS, 3DMAX, Sketchup and other software can be

162 imported to construct 3D scenes. The models created can also be exported to various common 3D model formats.

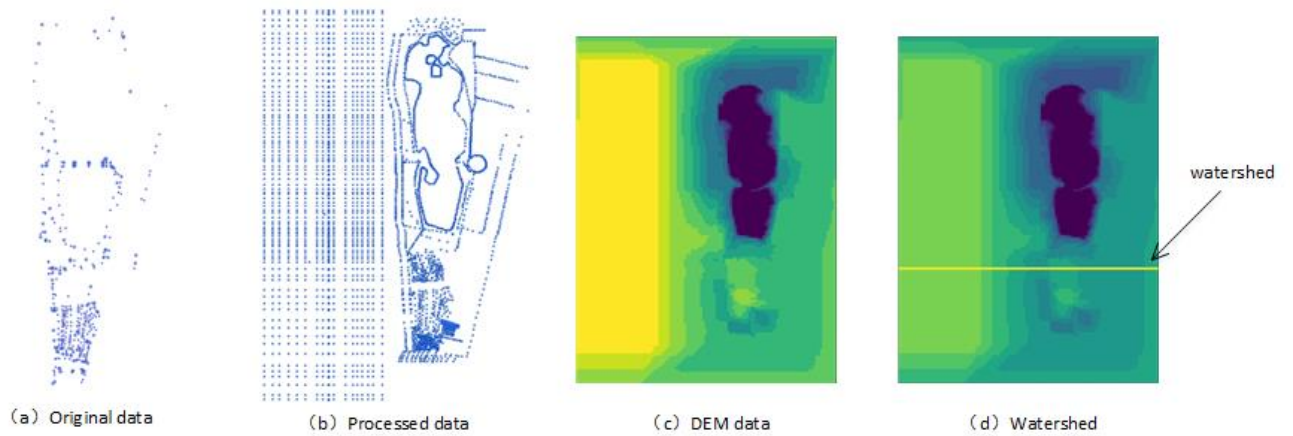
163 (3) It is suitable for the scene modeling within the city scope, but not for the detailed modeling of a single model.

164 Cesium is an open source 3d virtual Earth engine based on JavaScript. Cesium is designed to provide users with
165 powerful map data display and related operations. Cesium can run in browser supported by the WebGL. In this paper, the
166 Cesium is used to load the 3D model built by CityEngine, and its water surface simulation function is used to simulate the
167 regional waterlogging disasters under rainstorm scenarios in different recurrence periods.

168 3. Application examples

169 3.1 Elevation data

170 Elevation data processing mainly includes interpolation processing, automatic watershed extraction and sub-catchment
171 area division. The processing results are shown in Figure 7.



173 **Figure 7. Results of processing the DEM data**

174 The final results of watershed extraction are shown in the figure 6 (d). It divides the study area into two sub-catchment
175 areas. The field observation shows that the division result of the sub-catchment area is coincide with the actual topographic
176 features. The dividing line is a main road in the study area, which divides the study area into two sub-catchment areas of
177 north and south region.

178 3.2 Data of waterlogging simulation

179 3.2.1 Rainfall information

180 According to the standards of Wuhan drainage and waterlogging prevention system, the intensity of short duration
181 rainstorm in Wuhan should be calculated by the following formula:

$$182 \quad P = 0.5 \sim 10a \quad q = \frac{885[1 + 1.58 \lg(P + 0.66)]}{(t + 6.37)^{0.604}} \quad (8)$$

$$183 \quad P = 10 \sim 50a \quad q = \frac{577(1 + 0.96 \lg P)}{(t + 2.26)^{0.432}} \quad (9)$$

$$184 \quad P = 100a \quad q = \frac{1057}{(t - 0.57)^{0.317}} \quad (10)$$

185 Where: Q is the intensity of the storm, $L/s \cdot hm^2$; P is the designed rainfall recurrence period, a ; T is rainfall duration,
 186 min .

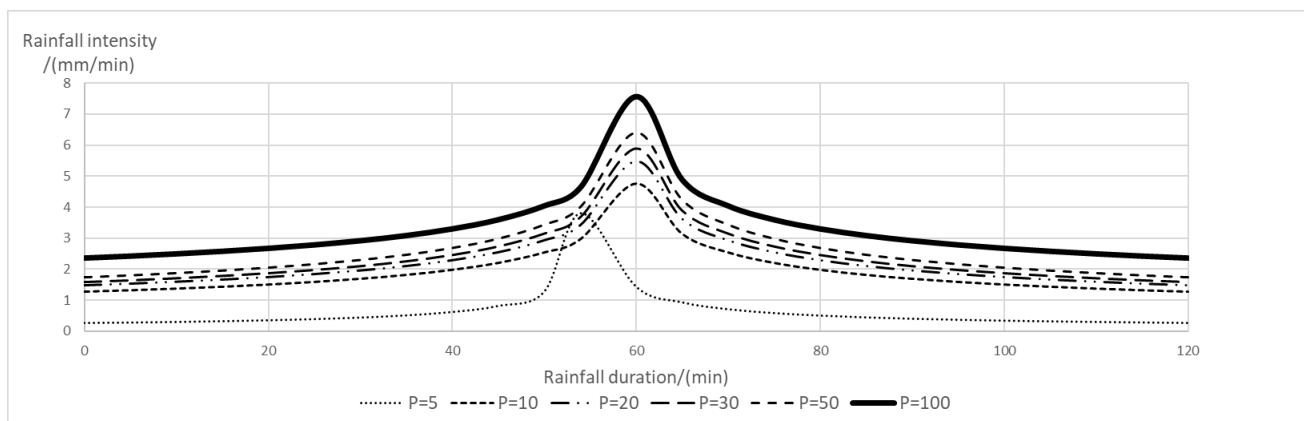
187 The short-duration rainstorm is expressed by the rainstorm intensity formula and the rain peak coefficient. When the
 188 rainstorm recurrence period is 5-10a, the rain peak coefficient is 0.45. When the rainstorm recurrence period is greater than
 189 10a, the rain peak coefficient is 0.5.

190 According to the Wuhan rainstorm intensity formula and the rain peak coefficients in different recurrence periods, the
 191 rainfall intensity process lines and rainfall amounts of $5a, 10a, 20a, 30a, 50a$ and $100a$ can be calculated. Take 2 hours for
 192 example, and the rainfall and average rainfall intensity at different recurrence periods were shown in Table 2.

193 **Tab.2 Rainfall and intensity with different rainfall recurrence**

| Return period (a) | rainfall intensity (mm) | Average rainfall intensity (mm/min) |
|-----------------------|-----------------------------|---|
| 5 | 75.02 | 0.625225349 |
| 10 | 102.10 | 0.8508956 |
| 20 | 117.16 | 0.976354424 |
| 30 | 125.96 | 1.049743131 |
| 50 | 137.06 | 1.142201968 |
| 100 | 166.59 | 1.388268252 |

194 The rainfall line in different recurrence periods is shown in Figure 8. As can be seen from the figure, the peak value
 195 of rainfall intensity usually occurs in about 60 minutes, and the maximum value of rainfall intensity in 5a recurrence is
 196 about $3.79 \text{ mm}/min$. With the increase of recurrence period, the peak value also increases continuously. The maximum
 197 value of rainfall intensity once in 100 years is about $7.57 \text{ mm}/min$.



198 **Figure 8. Rainfall process lines at different recurrence stages**

199 According to the SCS runoff model, the land types in the study area are divided into four types: urban land, road land,
 200 grassland and lake. The boundary of different land types in the study area are sketched by CAD. And the areas of different
 201 land types are classified and counted. Different type's area and value of CN are shown in Table 3.

202 **Tab.3 Statistical data of different land types**

203

| Catchment area | Land types | Area occupied | CN |
|----------------|-------------|---------------|----|
| North area | Urban land | 0.32 | 81 |
| | Street land | 0.22 | 85 |
| | Grass land | 0.13 | 58 |
| | Lake | 0.11 | 98 |
| | Total | 0.78 | |
| South area | Urban land | 0.15 | 81 |
| | Street land | 0.10 | 85 |
| | Grass land | 0.08 | 58 |
| | Total | 0.33 | |

204

3.2.2 Drainage information

205

206

207

208

209

3.2.3 Submergence depth calculation

210

211

212

213

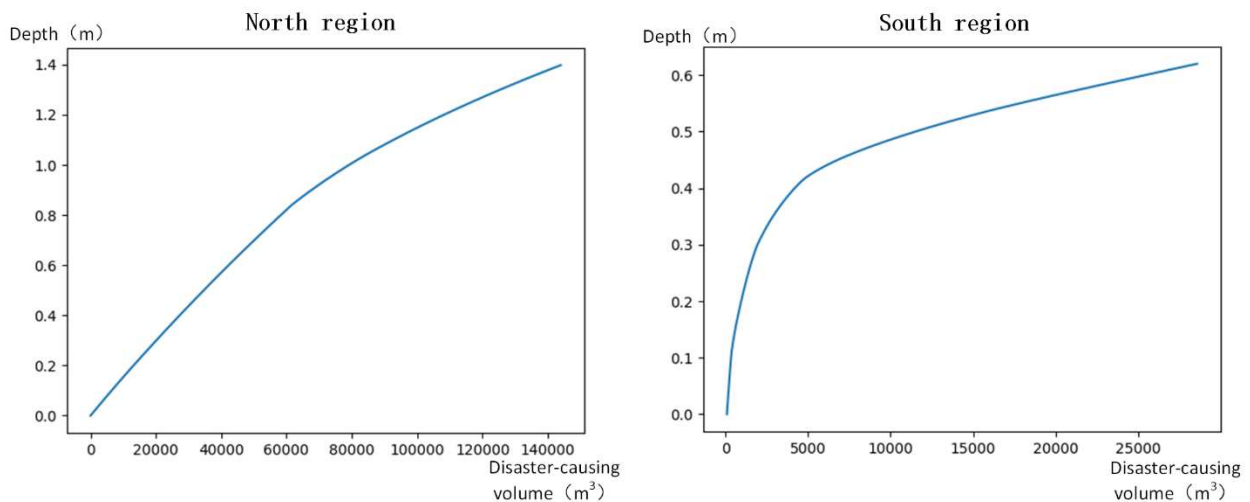
214

215

216

Because the study area is a small, the pumping and drainage capacity of the pumping station is not considered and only take pip drainage into consider. According to the design standard of Wuhan drainage and waterlogging prevention system, the design standard of Wuhan urban drainage pipe network is "once a year", and the drainage capacity is 36 mm/h.

On the basis of high-precision DEM data and urban waterlogging disaster model, the relation curve between disaster-causing volume and inundation depth is calculated as shown in Figure 9. It can be seen that when the disaster-causing volume is increasing, the submergence depth is increasing but the growth rate is gradually slowing down. This phenomenon is related to the topographic characteristics of the study area. There are several areas that are prone to flooding all the year around. At these place, with the continuous increase of the disaster-causing volume, the growth rate of the submerged area is far less than that of the disaster-causing volume, as well as with the continuous expansion of the submerged area, the growth rate of the submerged depth also slowed down.



217

218

Figure 9. Relationship between the amount causing waterlogging and depth

219

3.3 Geographic feature data

220 **3.3.1 Spatial data preparation**

221 The spatial data needed in the model mainly includes elevation data, building vector data and texture mapping. The
222 elevation data and building vector data is obtained by manual field measurement. The texture mapping is obtained by
223 camera. Part of the data is shown in Figure 10.



224
225 **Figure 10. Part of the spatial data**

226
227 **3.3.2 Spatial data preparation**

228 3D scene modeling is carried out according to the acquired spatial data, and the scene effect is shown in Figure 11.



229
230 **Figure 11. 3D scene simulation of the ZUEL campus**

231 **3.4 Waterlogging disaster simulation**

232 The urban waterlogging disaster simulation of different rainfall conditions is made on the 3D DEM model. And the
233 results are shown in Table 4, which are the rainstorm waterlogging simulations of the return period of 5, 10, 20, 30, 50 and
234 100 years with 2 hours' rainfall duration.

235 **Tab. 4 The rainstorm waterlogging simulations of different return periods**

| Catchment area | Return period (a) | Disaster amount (m ³) | Submergence depth (m) |
|----------------|-------------------|-----------------------------------|-----------------------|
| North area | 5 | 20772.5598 | 0 |
| | 10 | 41894.32683 | 0 |
| | 20 | 53636.92625 | 0.10 |
| | 30 | 60505.94465 | 0.17 |
| | 50 | 69159.91425 | 0.28 |
| | 100 | 92191.36053 | 0.46 |

| | | | |
|-------------------|-----|-------------|------|
| South area | 5 | 659.2633906 | 0.20 |
| | 10 | 9594.218553 | 0.53 |
| | 20 | 14561.81857 | 0.57 |
| | 30 | 17467.74055 | 0.60 |
| | 50 | 21128.81822 | 0.62 |
| | 100 | 30872.45303 | 0.68 |

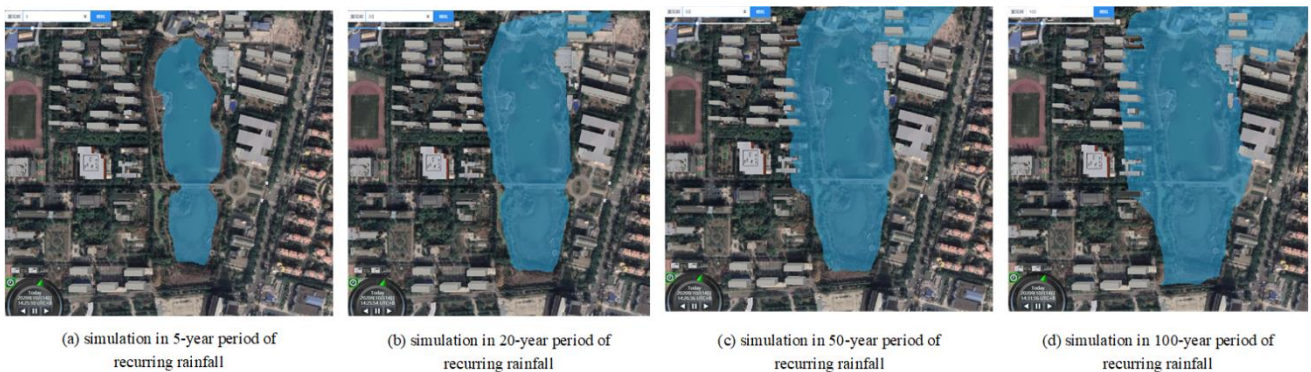
236

237 Figures 12 and 13 show the waterlogging scenarios of the north and south catchment area of the ZUEL campus by
 238 using the 3D visualization technology. The analysis is based on the results of 3D simulation and calculation.

239 When the rainfall return period is less than 20 years, the lake in north catchment area has good storage capacity which
 240 can protect the area from waterlogging disaster. But when the return period increases to 20 years, the waterlogging area
 241 takes the lake as the center and spreads to the surrounding area. Waterlogging begins to occur in the area. With the increase
 242 of years of return period, the waterlogging area increase rapidly while the submergence depth is low, which cause very little
 243 damage.

244 In the south catchment area, there is a local low topography, which leads to the waterlogging disaster even the rainfall
 245 period is 5 years. And the waterlogging area is relatively concentrated and small.

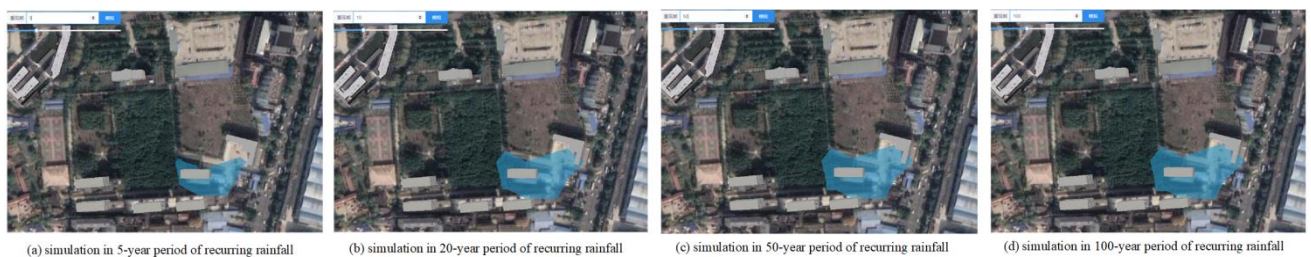
246 With the increase of years of return period, the increase of waterlogging area is not obvious but the submergence depth
 247 increases greatly. In the 100-year disaster simulation, the disaster situation in the south area is more serious than that in the
 248 north area. The simulation results are basically consistent with the waterlogging disaster caused by the 100-year- recurrence
 249 heavy rain in Wuhan in 2016.



250

251

Figure 12. The waterlogging scenarios of the north catchment area of the ZUEL campus



252

253

Figure 13. The waterlogging scenarios of the south catchment area of the ZUEL campus

254 **4. Conclusions**

255 Based on the previous studies and high-precision terrain data, the 3D DEM model is built in this paper to simulate the
256 urban waterlogging disasters under different recurrence stages of rainfall scenarios. The region survey is focused on the
257 campus of Zhongnan University of Economics and Law. The main conclusions are as follows:

- 258 • The model can effectively improve the simulation accuracy of waterlogging disaster. It can help to locate the
259 disaster area accurately, and directly display the submergence range and depth of waterlogging disaster by using
260 the 3D visualization technology. With the improvement of computer performance and the accuracy of measuring
261 equipment, the research on urban waterlogging disaster tends to small regions. The study in this paper can provide
262 an idea and method for the research on urban waterlogging disaster.
- 263 • The basis of waterlogging disaster simulation in this paper is to use the watershed extraction method to delimit
264 the Sub-catchment area according to the high-precision DEM model of urban topography and geomorphology.
265 The results are consistent with the actual terrain, which shows that the watershed extraction method is more
266 suitable for waterlogging simulation in a small area than Manual Partition, Tyson Polygon Partition or Drainage
267 Network Partition.
- 268 • The urban waterlogging disaster simulate model is built with in combination with the rainstorm intensity formula
269 and SCS model of runoff simulation. The urban drainage network is simplified in this model, which can make
270 the simulation calculation much easier but not affect the reliability of the results. This feature makes this model
271 more suitable for waterlogging disaster simulation in urban areas without enough pipe network data.
- 272 • The waterlogging simulate method provide in this paper is easy to extend to other areas such as reservoir, tailings
273 pond.

274

275 **Reference**

- 276 [1] Shi L, Ling F, Foody G M, et al. Permanent disappearance and seasonal fluctuation of urban lake area in Wuhan, China
277 monitored with long time series remotely sensed images from 1987 to 2016[J]. *International Journal of Remote*
278 *Sensing*, 2019, 40(22): 8484-8505.
- 279 [2] Suhyung Jang, Minock Cho, Jaeyoung Yoon, Yongnam Yoon, Sangdan Kim, Geonha Kim, Leehyung Kim, Hafzullah
280 Aksoy. Using SWMM as a tool for hydrologic impact assessment[J]. *Desalination*, 2007, 212(1).
- 281 [3] Zhu, Dongdong, Nianqing Zhou, and Simin Jiang. "Research overview of runoff model for urban rainwater." *J Water*
282 *Resour Water Eng* 22 (2011): 132-137.
- 283 [4] Garcia D F L. Simulation of Urban Runoff for Permeable Pavements through Storm Water Management Model
284 Software: Case Study in Facatativa in Colombia[J].
- 285 [5] Qiu, Jin-wei, et al. "The simulation system for heavy rainfall in Tianjin City." *Journal of Hydraulic Engineering* 11
286 (2000): 34-42.
- 287 [6] Li, N., J-W. Qiu, and X-T. Cheng. "Study on simulation system of rainstorm waterlogging in Tianjin City." *Journal of*
288 *Natural Disasters* 11.2 (2002): 112-118.
- 289 [7] WANG L, QIN Q, LI J, et al. Study on the disaster analysis modal of water-logging in city based on CIS [J][J]. *Science*
290 *of Surveying and Mapping*, 2004, 3.
- 291 [8] Ye L M, Zhou Y H, Xiang H, et al. Risk regionalization of urban roads waterlogging disasters based on GIS rainstorm
292 flood inundation model[J]. *Resour Environ Yangtze Basin*, 2016, 25(6): 1002-1008.
- 293 [9] Jing Y, Yin Z, Yin J, et al. GIS-based analysis on rainstorm waterlogging hazards in Pudong new area in Shanghai[J].
294 *J. Catastrophol*, 2010, 25: 58-63.
- 295 [10] Yin Z E, Xu S Y, Yin J, et al. Small-scale based scenario modeling and disaster risk assessment of urban rainstorm
296 water-logging[J]. *Acta Geographica Sinica*, 2010, 65(5): 553-562.
- 297 [11] Yin, Jie, Shiyuan Xu, and Jiahong Wen. "Community-based scenario modelling and disaster risk assessment of urban
298 rainstorm waterlogging." *Journal of Geographical Sciences* 21.2 (2011): 274-284.
- 299 [12] Han G, Kaspersen R E. Dilemmas and pathways to dealing with flood problems in twenty-first century China[J].
300 *International journal of disaster risk science*, 2011, 2(3): 21-30.
- 301 [13] Rahman M S, Di L, Yu E, et al. Remote Sensing Based Rapid Assessment of Flood Crop Damage Using Novel Disaster
302 Vegetation Damage Index (DVDI)[J]. *International Journal of Disaster Risk Science*, 2020: 1-21.
- 303 [14] Meng X, Zhang M, Wen J, et al. A simple GIS-based model for urban rainstorm inundation simulation[J].
304 *Sustainability*, 2019, 11(10): 2830.
- 305 [15] Zhou, Jingyi, et al. "Spatio-Temporal Visualization Method for Urban Waterlogging Warning Based on Dynamic

306 Grading." ISPRS International Journal of Geo-Information 9.8 (2020): 471.

307 [16] Costabile P, Costanzo C, De Lorenzo G, et al. Terrestrial and airborne laser scanning and 2-D modelling for 3-D flood
308 hazard maps in urban areas: new opportunities and perspectives[J]. Environmental Modelling & Software, 135:
309 104889.

310 [17] Su, Boni, Hong Huang, and Yuntao Li. "Integrated simulation method for waterlogging and traffic congestion under
311 urban rainstorms." Natural Hazards 81.1 (2016): 23-40.

312 [18] Quan, Rui-Song. "Rainstorm waterlogging risk assessment in central urban area of Shanghai based on multiple
313 scenario simulation." Natural hazards 73.3 (2014): 1569-1585.

314 [19] WANG, La-chun, et al. "The simulation and prediction of economic loss of flood and waterlogging in Taihu Lake
315 Basin." JOURNAL OF NATURAL DISASTERS 9.1 (2000): 33-39.

316 [20] Wu Y, Peng F, Peng Y, et al. Dynamic 3D Simulation of Flood Risk Based on the Integration of Spatio-Temporal GIS
317 and Hydrodynamic Models[J]. ISPRS International Journal of Geo-Information, 2019, 8(11): 520.

318 [21] Lianbing D, Daming L, Zhiming C. Emergency management system of urban waterlogging based on cloud computing
319 platform and 3D visualization[J]. Journal of Intelligent & Fuzzy Systems, 2020 (Preprint): 1-14.

320 [22] Kim M, Song K, Chon J. Key coastal landscape patterns for reducing flood vulnerability[J]. Science of The Total
321 Environment, 2020: 143454.

322 [23] Seenu P Z, Rathnam E V, Jayakumar K V. Visualisation of urban flood inundation using SWMM and 4D GIS[J].
323 Spatial Information Research, 2019: 1-9.

324 [24] Lin W, Sun Y, Nijhuis S, et al. Scenario-based flood risk assessment for urbanizing deltas using future land-use
325 simulation (FLUS): Guangzhou Metropolitan Area as a case study[J]. Science of The Total Environment, 2020:
326 139899.

327

Figures



Figure 1

The condition of waterlogging in 2016

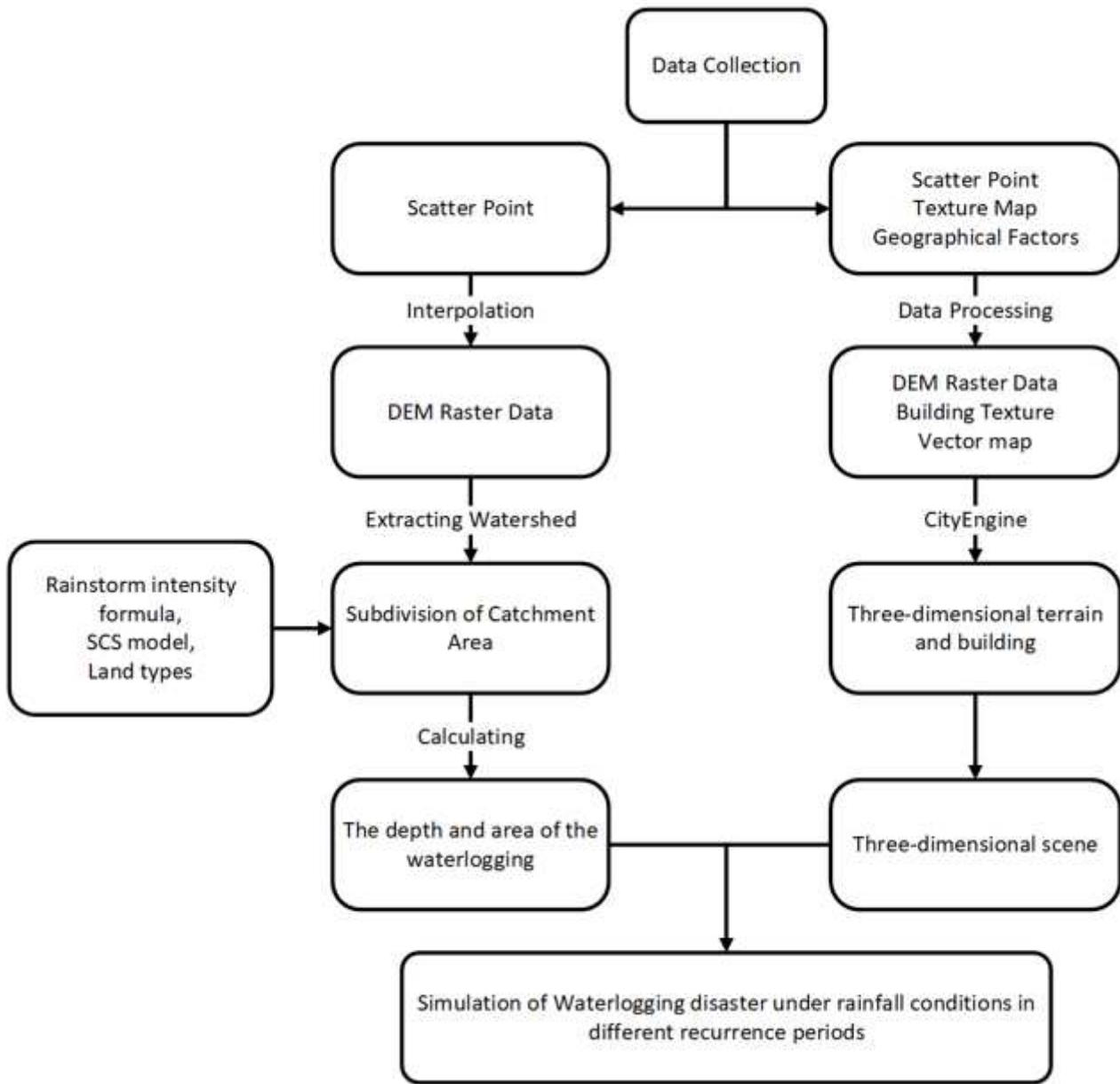


Figure 2

Framework of waterlogging simulation

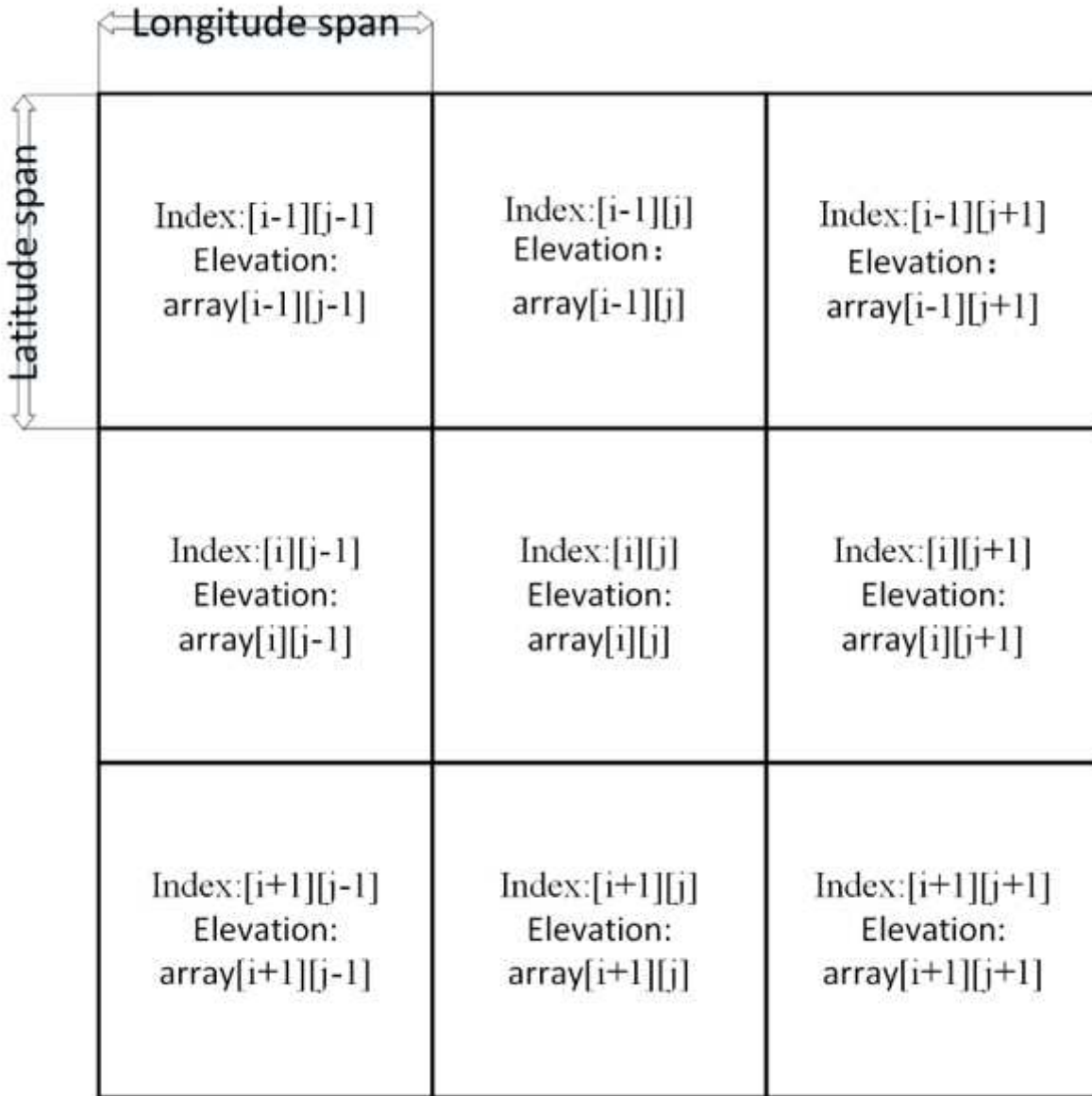


Figure 3

Principle of grid data

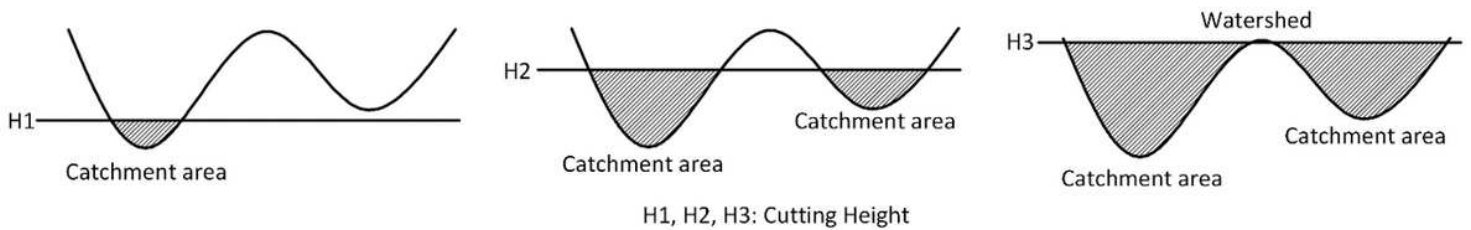


Figure 4

Principle of extracting watershed

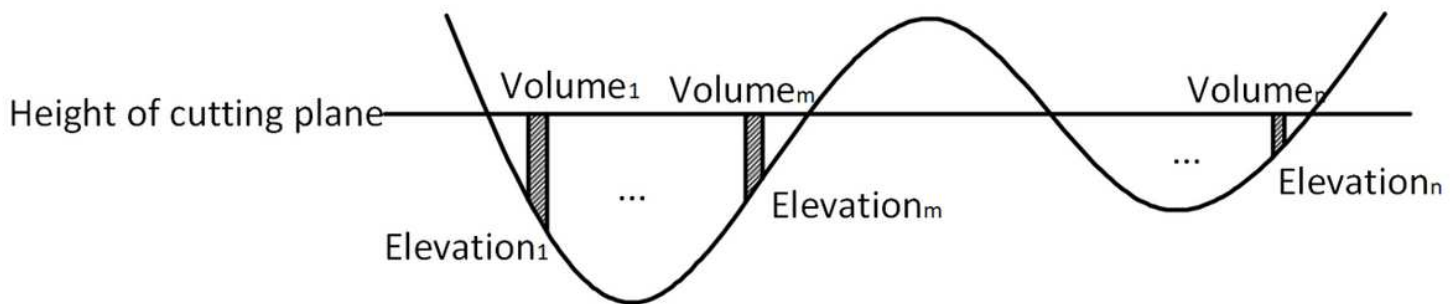


Figure 5

Principle of calculating the volume of DEM data

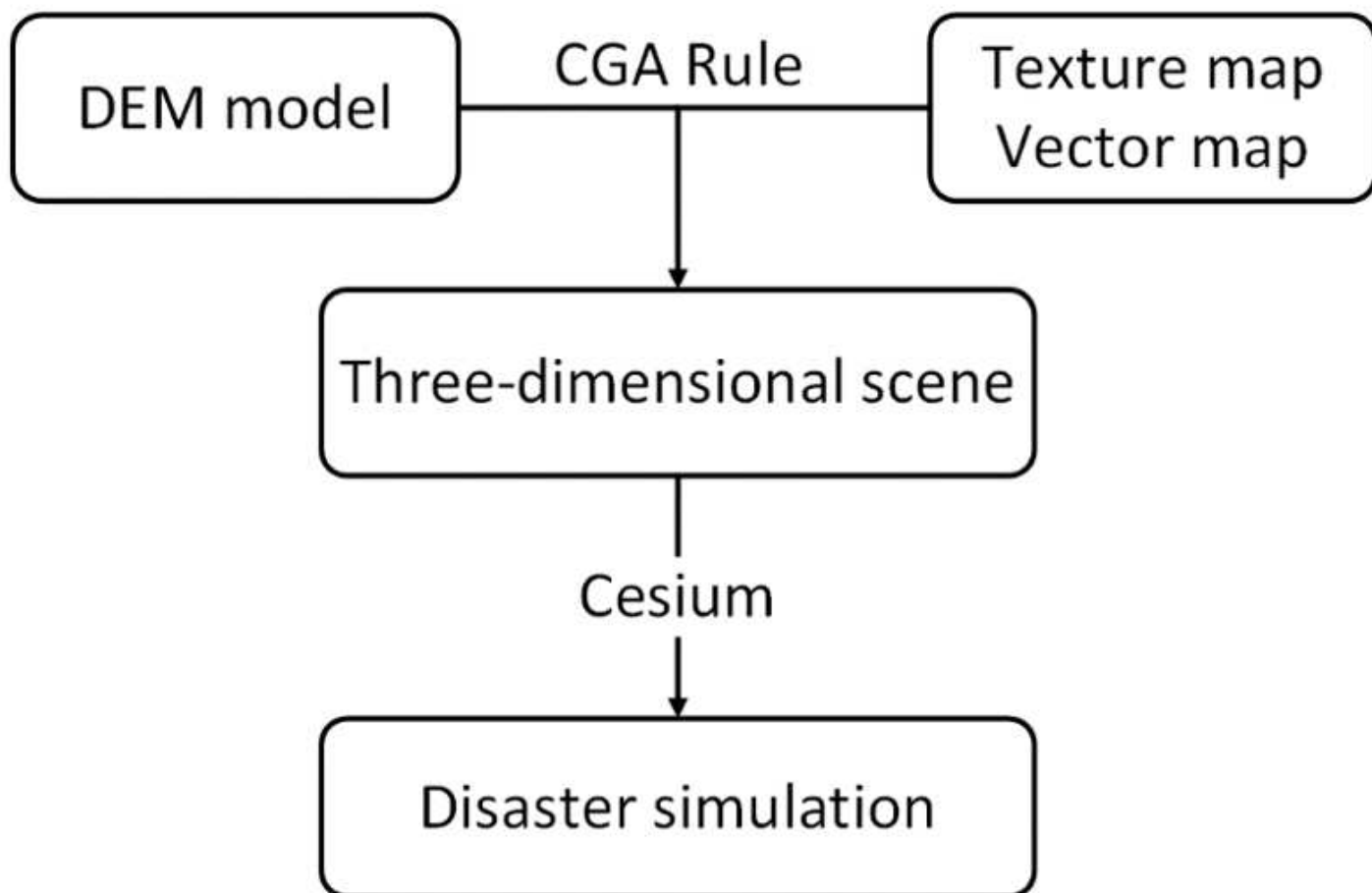


Figure 6

Framework of 3-dim visualization

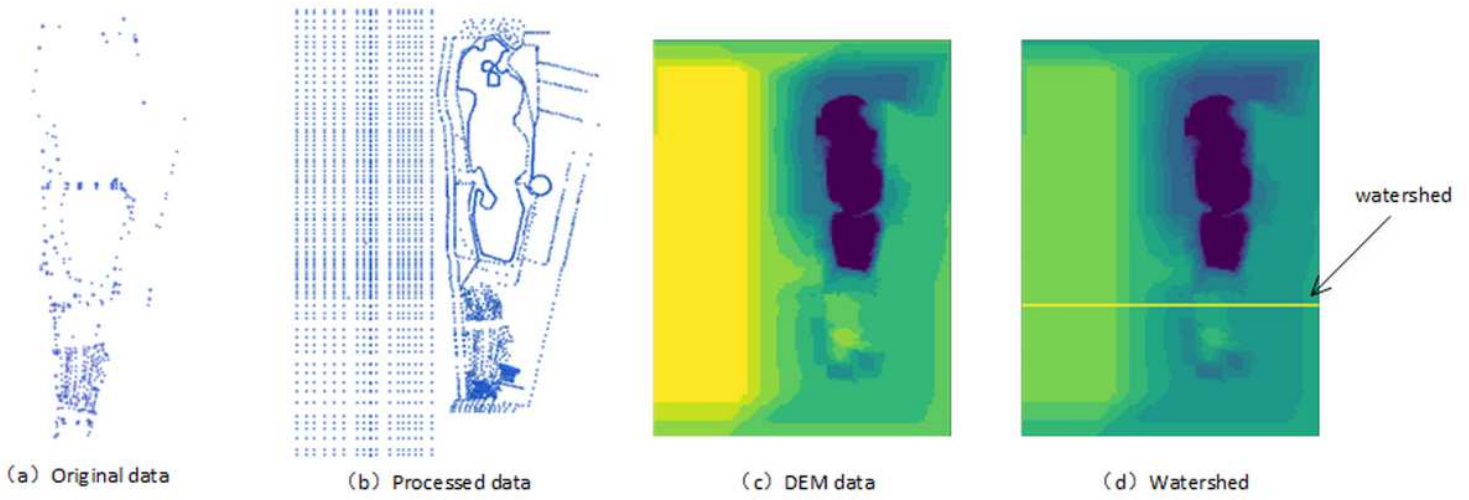


Figure 7

Results of processing the DEM data

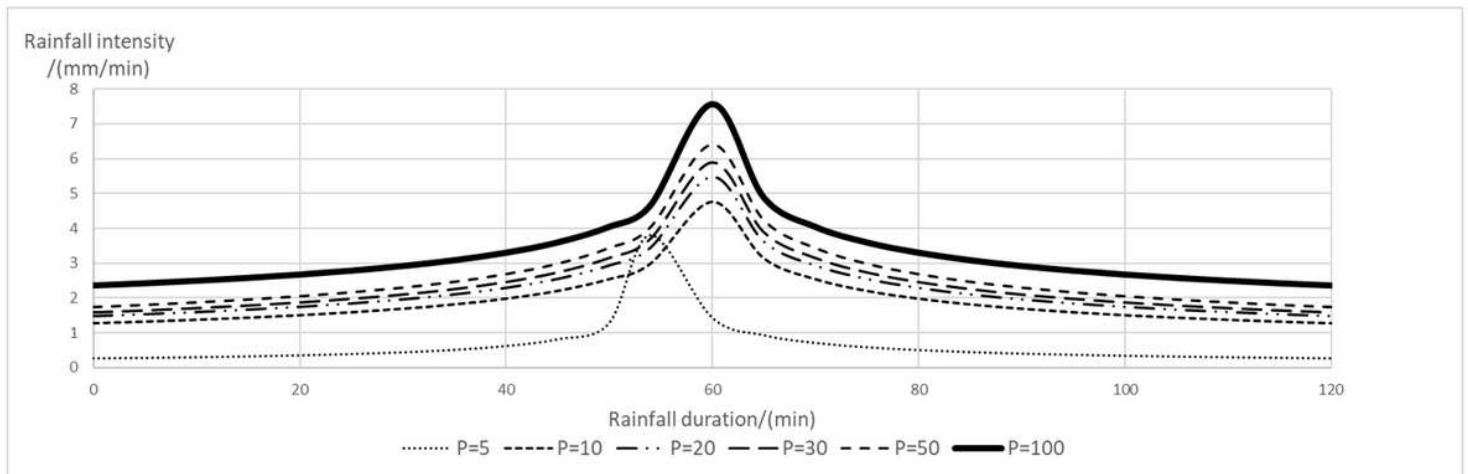


Figure 8

Rainfall process lines at different recurrence stages

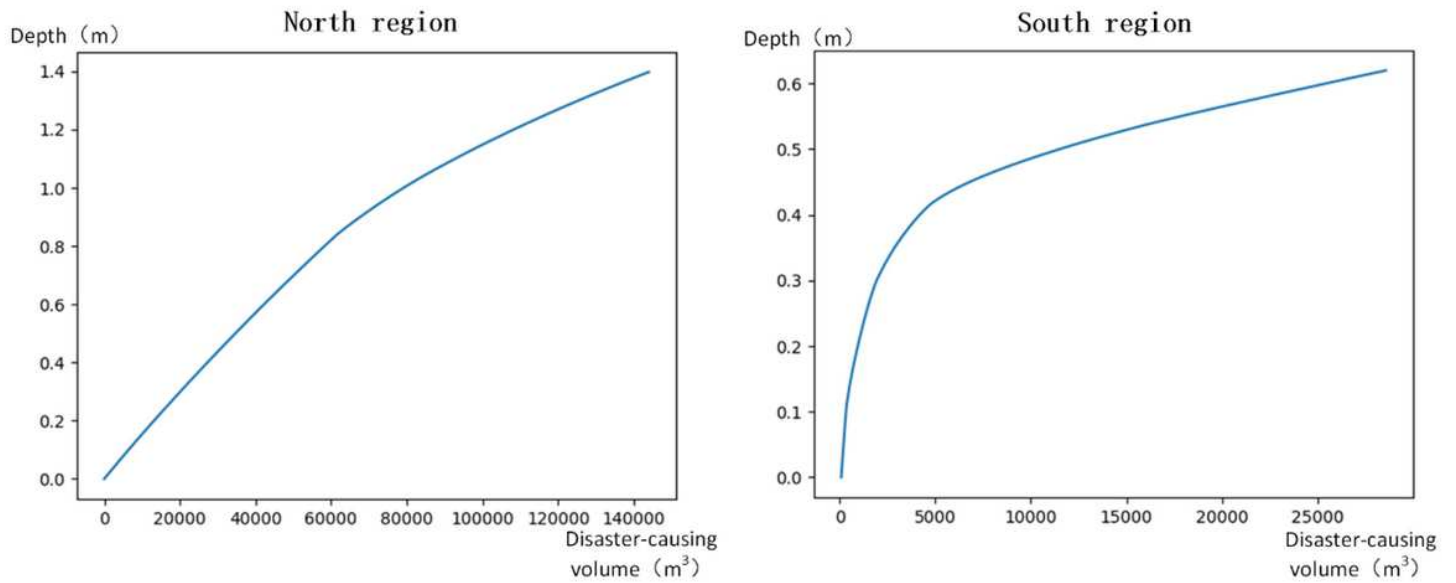


Figure 9

Relationship between the amount causing waterlogging and depth



Figure 10

Part of the spatial data

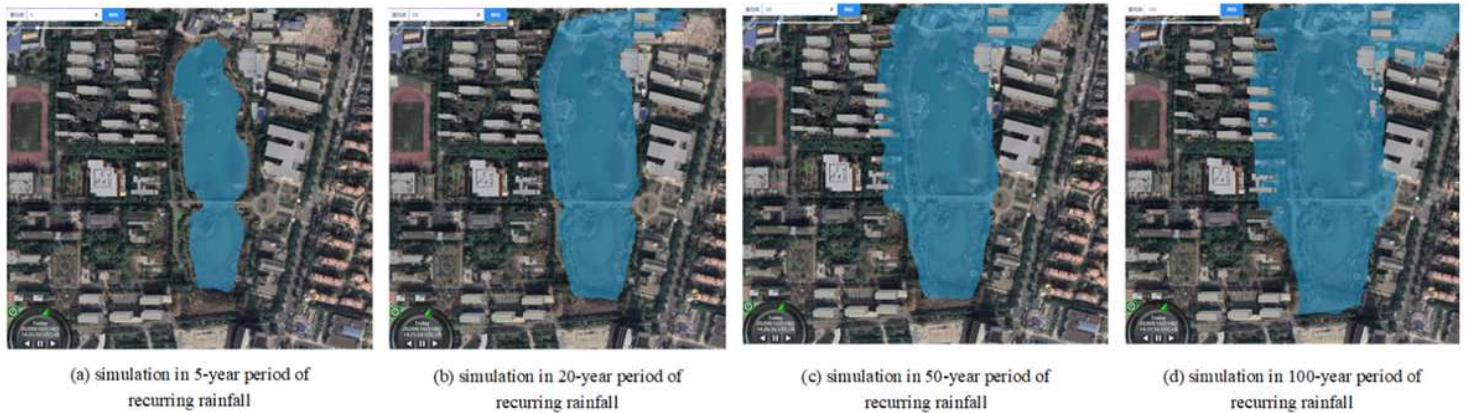


Figure 12

The waterlogging scenarios of the north catchment area of the ZUEL campus

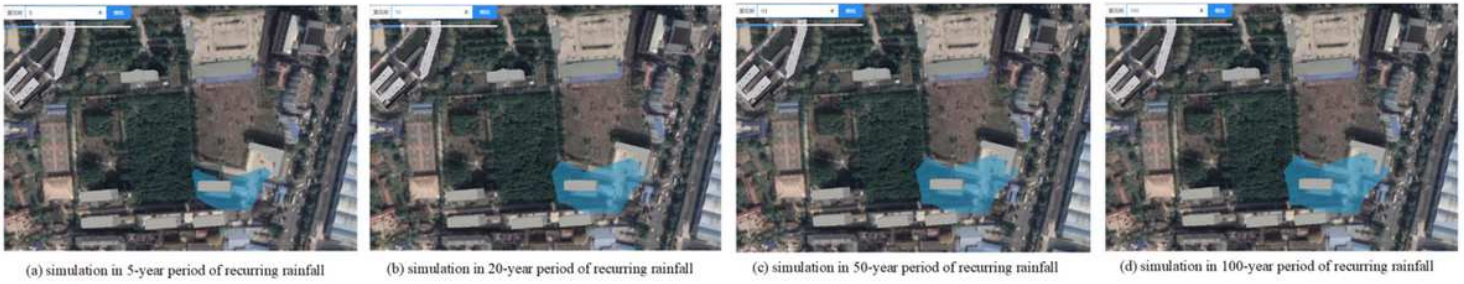


Figure 13

The waterlogging scenarios of the south catchment area of the ZUEL campus